Session 7:

Star Formation:

Tracers, Scaling Relations, Efficiency, Modeling

https://doi.org/10.1017/S1743921313001464 Published online by Cambridge University Press

Molecular Gas, Dust, and Star Formation in Galaxies
Proceedings IAU Symposium No. 292, 2012
T. Wong & J. Ott, eds.

doi:10.1017/S1743921313001464

[FeII] as a shock tracer in NGC 253

Marissa J. F. Rosenberg, Paul P. van der Werf and Frank P. Israel

Leiden Observatory, Universiteit Leiden,
NL-2300CA, Leiden, the Netherlands
email: rosenberg@strw.leidenuniv.nl

Abstract. Supernovae play an integral role in the feedback of processed material back into the interstellar medium (ISM) of galaxies and are responsible for most of the chemical enrichment of the universe. The rate of supernovae can also reveal the star formation histories. In a sample of 11 nearby galaxies observed with SINFONI, a strong linear correlation between $[FeII]_{1.26}$ luminosity and Starburst 99-derived supernova rate is found on a pixel-pixel basis. In the very nearby archetypal starburst galaxy NGC 253, the excitation of molecular gas is a subject of debate. Using the correlation between [FeII] and supernova rate, we can determine if supernovae can account for the excitation of the bright observed near-infrared H_2 emission.

Keywords. supernovae: general — instrumentation: high angular resolution — galaxies: individual (NGC 253)

1. Introduction

The supernova rate (SNrate) is typically estimated by the integrated non-thermal radio continuum emission. Near-infrared (NIR) observations of supernova remnants (SNR) often show strong [FeII] emission line flux coincident with the radio peak. Iron atoms are typically locked in dust grains and shock fronts of the SNR cause efficient grain destruction through thermal sputtering. This releases the iron into the gas-phase where it is singly ionized by the interstellar radiation field, making [FeII] a strong tracer of shocks, which are often caused by expanding SNR.

Using SINFONI observations of 11 near-by galaxies, Rosenberg *et al.* (2012) performed a pixel-by-pixel analysis of the correlation between $[FeII]_{1.26}$ emission and SNrate. The Brγ line flux along with the K band continuum was used to find the equivalent width of Brγ, which was then used as input into the SB99 model to estimate the age of each pixel. From age, SB99 provides a SNrate, normalized to an initial mass of $10^6 M_\odot$. The normalized SNrate is scaled by ionizing photon flux (proportional to Brγ luminosity), to derive the true SNrate in each pixel.

Comparing the $[FeII]_{1.26}$ luminosity map to the Starburst 99-derived SNrate map reveals striking morphological similarities. In addition, this correlation is further evident quantitatively, comparing [FeII] luminosity and SNrate on a pixel-pixel basis (Figure 1).

One of the best laboratories to study the excitation mechanisms and drivers of starburst galaxies in detail is NGC 253. This galaxy is a nearby (3.5 Mpc), edge-on infrared bright galaxy that is part of the Sculptor group. It is classified as a late-type barred spiral galaxy (SAB(s)c) with star formation confined to the inner 0.5 kpc. The star formation rate of the starburst is 1.4-9.5 $M_\odot$ yr^{-1}. This intense episode of star formation is driven by a 7 kpc bar, which funnels gas into the nucleus (Engelbracht *et al.* 1998).

The subject of excitation mechanisms has been extensively studied in NGC 253. Martin *et al.* (2006) finds that the chemistry and heating of NGC 253 is dominated by large scale, low velocity shocks. Presence of shocked molecular material is indeed evident through the presence of widespread SiO emission throughout the nuclear regions (Garcia-Burillo

et al. 2000). Martin *et al.* (2009) suggest that, although NGC 253 is dominated by shock chemistry, PDRs play a crucial role in the chemistry, since there are very high abundances of PDR tracing molecules, namely HCO^+, CO^+. Harrison *et al.* (1998) used the ortho- to para- ratio of H_2, to argue that most of the H_2 is excited by PDRs instead of shocks.

Since shocks often originate from supernovae, we can use the $[FeII]_{1.26}$ and SNrate correlation, along with other diagnostic tracers to constrain the excitation mechanism of the near infrared H_2 emission in NGC 253.

2. Shocks vs. Fluorescence

The K band continuum map and H_2 1-0 S(1), Brγ, and $[FeII]_{1.64}$ emission line maps are shown in Figure 2. All line maps are plotted with respect to the kinematic center proposed by Muller-Sanchez *et al.* (2010). We have chosen 8 regions defined by the most dominant H_2 peaks and these regions are overplotted by white rectangles in each map. There is an additional region centered on the kinematic center. All regions are 12×12 pixels or 1.5×1.5 arcseconds.

The NIR is rich with ro-vibrational H_2 lines, which can either be excited thermally, through shocks, or by fluorescence, through the absorption of UV photons from O and B stars. In the case of shock excited H_2 emission, the gas is thermalized and the energy levels are populated in a "bottom-up" manner. The resulting gas temperature is around 1000 K and thus there is little H_2 emission from the $v \geqslant 3$ states, which have excitation temperatures above 15,000 K. However, in the case of excitation by UV photons, the H_2 molecule absorbs a highly energetic photon and is excited to an upper electronic energy level and then proceeds to cascade downwards. This is considered populating the energy levels from the "top-down", which results in exciting higher H_2 energy levels.

In order to determine which excitation mechanisms are dominating which regions, we can use the information from the Brγ and [FeII] tracers. Specifically, if the H_2 is undergoing excitation by UV photons in a dense environment, this region should also be bright in Brγ emission. Conversely, if the H_2 is being excited by shocks, then the [FeII] emission will also be bright in this region.

In order to determine the excitation mechanism responsible for the NIR H_2 emission, we compare the morphology of the H_2 map to that of the [FeII] map and the Brγ map. The $[FeII]_{1.64}$ map reveals emission peaking near, but not coincident with Region 4, the H_2 peak. In the northeastern regions, the [FeII] emission is also clumpy, with some of the clumps coinciding with the H_2, such as Regions 5, 7 and 8. However, in

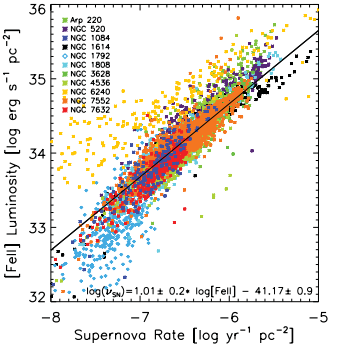

Figure 1. A pixel-pixel plot of SNrate, as derived from SB99, compared to [FeII] luminosity. Each galaxy is represented with a different color and the values are normalized to 1 square parsec. The black line represents the best fit powerlaw excluding NGC 1792.

https://doi.org/10.1017/S1743921313001464 Published online by Cambridge University Press

general the H_2 emission shares few morphological similarities to the [FeII] emission. From Rosenberg *et al.* (2012) we can calculate the SNrate from the FeII luminosity. Our integrated supernova rate, throughout the galaxy, is 0.2 SN yr^{-1}, which is well matched to previous supernova rate measurement of 0.1-0.3 (Ulvestad & Antonucci 1997). The lack of correlation between the [FeII] and H_2 morphologies along with the low SNrate across the galaxy suggests that shocks originating from supernovae are not very important to the H_2 excitation.

Similarly, comparison of the H_2 and the Brγ map reveals little correlation. The Brγ flux peak is coincident with the super star cluster (Region 2), but shows no clear flux increase near Region 4, where H_2 is brightest. The Brγ is also generally less extended than the H_2, with most of the emission in the southwestern portion of the galaxy, centered on the super star cluster. Thus, the source of Brγ excitation is not the same as that exciting the H_2. However, Brγ only traces the most massive and young O stars. For Brγ emission, the star must emit Lyman continuum photons ($\lambda < 912$ Å, 13.6 eV), yet H_2 is excited by $\lambda < 1100$ Å (11.2 eV).

Like H_2, polycyclic aromatic hydrocarbons (PAHs) have a lower excitation energy than HI ($\lambda \sim 4200$ Å for $N_C > 50$), where N_C is the number of carbon atoms, thus are excited not only by O stars but also by slightly less massive, B-type stars. Therefore, the PAH emission traces the more general fluorescently excited material, including excitation by both O and B stars. In Figure 3, we compare the H_2 map to a PAH map from ISAAC 3.28 μm continuum subtracted map and find that the H_2 peaks are coincident with both

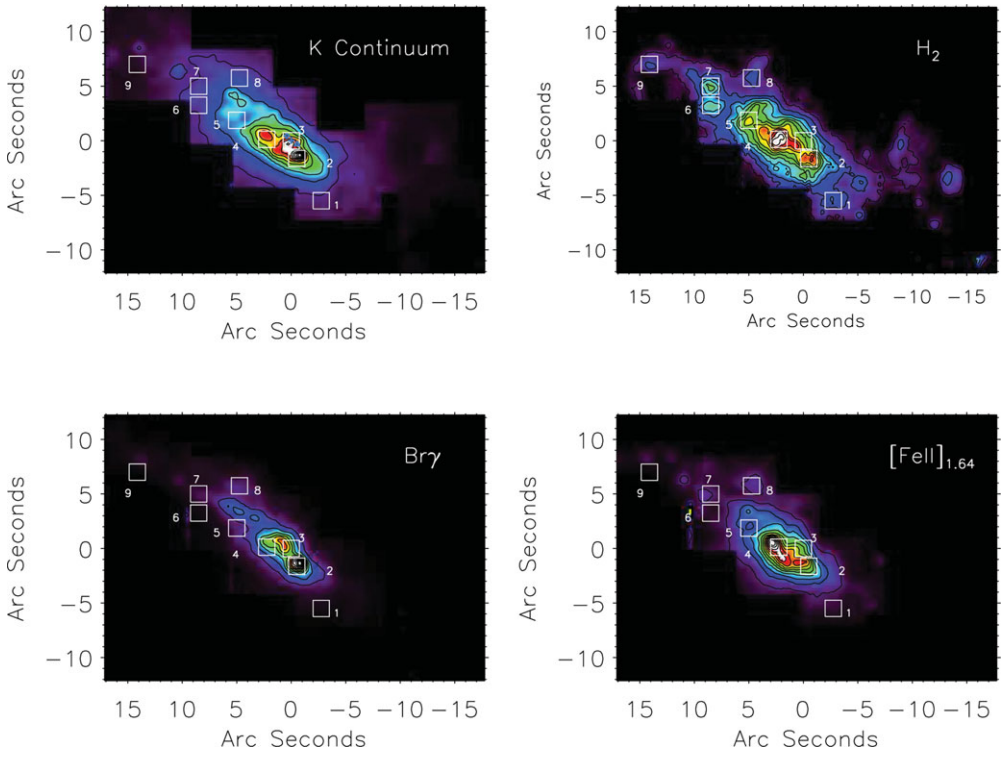

Figure 2. K band continuum map, H_2 1-0 S(1), Brγ, and $[FeII]_{1.64}$ line map of NGC 253. The offset from the kinematic center at position $(\alpha, \delta)_{2000} = (00^h47^m33^s.14, -25°17'17''.52)$ is given on each axis.

https://doi.org/10.1017/S1743921313001464 Published online by Cambridge University Press

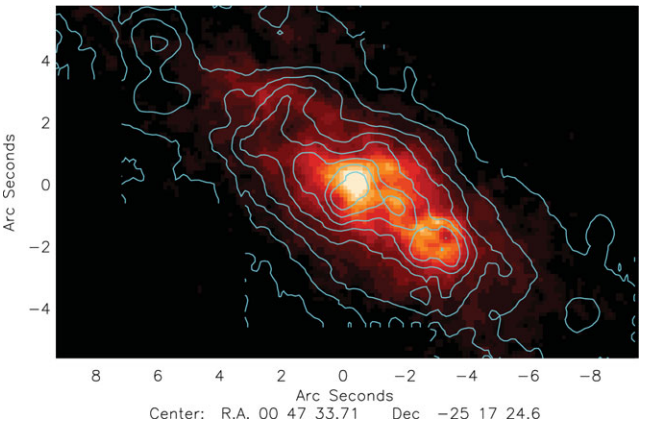

Figure 3. PAH 3.28 μm continuum subtracted image from ISAAC with H_2 1-0 S(1) contours.

the primary and secondary PAH peaks and the H_2 shares a generally similar morphology to that of the diffuse PAH emission.

The correlation between H_2 and PAH morphology suggests that most of the emission in NGC 253 is fluorescently excited. In addition, the correlation between the PAH and H_2 emission indicates that the H_2 is being excited by the same stars that are exciting the PAHs, mainly B-type stars. Using the 2-1 S(1)/1-0 S(1) ratio to distinguish between shock and fluorescently excited gas, we place an upper limit of 33% on the amount of shocked H_2 gas. Further evidence supporting fluorescent excitation as the dominant mechanism exciting the hot H_2 is confirmed using diagnostic excitation level diagrams and comparing our observations to PDR and shock models. Full details of this analysis can be found in Rosenberg *et al.* (in prep.).

References

Engelbracht, C. W., Rieke, M. J., Rieke, G. H., Kelly, D. M., & Achtermann, J. M. 1998, *ApJ*, 505, 639

Garcia-Burillo, S., Martin-Pintado, J., Fuente, A., & Neri, R. 2000, *ApJS*, 355, 499

Harrison, A., Puxley, P., Russell, A., & Brand, P. 1998, *MNRAS*, 297,624

Martin, S., Martin-Pintado, J., & Viti, S. 2009, *ApJ*, 706,1323

Martin, S., Mauersberger, R., Martin-Pintado, J., Henkel, C., & Garcia-Burillo, S. 2006, *ApJS*, 164, 450

Muller-Sanchez, F., Gonzalez-Martin, O., Fernandez-Ontiveros, J. A., Acosta-Pulido, J. A., & Prieto, M. A. 2010, *ApJ*, 716,1166

Rosenberg, M. J. F., Van der Werf, P. P. & Israel, F. P. 2012, *A&A*, 540, 116

Rosenberg, M. J. F., Van der Werf, P. P. & Israel, F. P. 2012, *A&A submitted*

Sternberg, A. & Dalgarno, A. 1989, *ApJ*, 338,197

Ulvestad, J. S. & Antonucci, R. R. J. 1997, *ApJ*, 716,1166

https://doi.org/10.1017/S1743921313001464 Published online by Cambridge University Press